Acta Med. Okayama, 2004
Vol. 58, No. 3, pp. 157-162

Acta Medica Okayama
http://www.lib.okayama-u.ac.jp/www/acta/

Original Article

Evaluation of Contour of Unruptured Cerebral Aneurysm Using Three-dimensional CT Cisternogram

Keisuke Onoda[a], Toru Satoh[b], Shoji Tsuchimoto[a]*, and Atsushi Katsumata[a]

[a]Department of Neurosurgery, Onomichi Municipal Hospital, Hiroshima 722-8503, Japan, and
[b]Department of Neurosurgery, Ryofukai Satoh Neurosurgical Hospital, Hiroshima 729-0104, Japan

Angiography is gold standard technique as preoperative examination for unruptured aneurysmal surgery. Neurosurgeons have observed the unexpected irregular shape and size of the aneurysmal dome and neck in many cases of unruptured cerebral aneurysms during aneurysmal microsurgery, and known the discrepancy between the findings of angiography and operative view. We could not find out the report described the preoperative evaluation of outer-wall (contour) of aneurysm. In the present study, we attempted to evaluate the outer-wall of an unruptured cerebral aneurysm using three-dimensional CT cisternogram (3D-CTC) to provide useful preoperative information. The study was performed on three cases of unruptured cerebral aneurysm that were identified incidentally by MR angiography. We performed three-dimensional CT aniography (3D-CTA) and 3D-CTC for each patient. In the present study, we visualized the contours of vessels and aneurysms using a 3D-CTC in three cases of unruptured cerebral aneurysm. We found the discrepancy between the 3D-CTC contour image and the intra-luminal image 3D-CTA image. This method may be useful for the decision of the surgical approach and have the potential to evaluate the anatomical structure of aneurysmal dome and neck preoperatively.

Key words: three-dimensional CT cisternogram, three-dimensional CT angiogram, unruptured cerebral aneurysm, contour of cerebral aneurym

Recently, MR angiography has been widely applied in screening examinations of cerebrovascular lesions, increasing the chances of detecting unruptured cerebral aneurysms. Unruptured cerebral aneurysms have a risk of rupture even when they are relatively small, so prophylactic surgical treatment is undergone in some cases [4, 8, 9]. Three-dimensional CT angiograms (3D-CTA) [2, 5], obtained by the intravenous administration of contrast medium, provide a pure intra-luminal filling image of the vessel and aneurysm, which is essentially different from the contour (outer wall) of the angioarchitecture of cerebral aneurysm encountered during surgery. In the present study, we performed a three-dimensional CT cisternogram (3D-CTC), which represented the real contour of the vessels and aneurysm.

Received October 7, 2003; accepted February 4, 2004.
*Corresponding author. Present Adderss: Department of Neurosurgery, Okayama University Graduate School of Medicine and Dentistry, Okayama 700-8558, Japan
Phone: +81-86-235-7336; Fax: +81-86-227-0191

Materials and Methods

The study was performed on 3 cases of unruptured cerebral aneurysm that were identified incidentally by MR angiography. Before the examinations, the informed consent was obtained from all patients. Each patient was positioned laterally, and 10 ml of non-ionic iodine contrast

medium (300 mgI/ml) (Omnipaque-300^{R}; Daiichi Pharmaceutical Co., Ltd., Tokyo, Japan) was injected into the spinal subarachnoid space via lumbar puncture. To introduce the contrast medium into the cranial basal cistern, the patients were settled into praying position with foreheads resting on the table for apporoximately 10 min, then eased back into a supine position. CTC was performed using a multi-detector row CT (HiSpeed Nx/is; General Electric-Yokogawa Medical Systems Co., Ltd., Tokyo, Japan). The protocol used was as follows: helical acquisition started with a 140-kV peak, 150 mA, 25-cm field of view, a 512 × 512 matrix, 1 mm collimation, detector in 2 rows, table speed of 0.8 mm/sec, and high quality mode (pitch 1.5). A total of 79 sections was obtained, each with a thickness of 1 mm. The data of the source axial images were reconstructed every 0.5 mm with a 10-cm field of view, and the data were then transferred to a workstation (Zio M900 3.0^{R}; AMIN Co., Tokyo, Japan). The 25 serial volume data, including the basal cistern, were selected, and were reconstructed to every 0.25 mm (50 volume data) on the workstation, then processed into a 3D volume rendering data set in 10 sec. A minimum intensity projection image was reconstructed from the data. Using a parallel volume rendering method [6, 7], the 3D-CTC was created by selecting the 3D data set from the opacity chart of CT values using a declining slope curve with a threshold range of 110 HU (100% opacity level) to 130 HU (0% opacity level), and represented the contour of the structures within the cistern. Additionally, transparent 3D-CTC was created by selecting the boundary between the cisternal structures and the cerebrospinal fluid, using a spiked peak curve with a threshold range of 110–130 HU (peak value at 120 with 100% opacity level, with 20 HU window width). The resulting transparent 3D-CTC represented the boundary of the vessels and aneurysmal walls as a series of rings, and provided an extensive transparent view of the cisternal structures with an adjacent overlying brain through the spaces between rings.

The 3D-CTA was performed using the same CT scanner, with the following protocol [7]: helical acquisition using 100 ml of nonionic iodine contrast medium with an iodine concentration of 320 mg/ml (Optiray 320 Syringe^{R}; Yamanouchi Pharmaceutical Co., Ltd., Tokyo, Japan) injected at a rate of 2 ml/sec into the antecubital vein with a power injector (Dynamic CT injector MCT320P; Medrad, Pittsburgh, PA, USA), with acquisition starting 21 seconds after the start of the injection. A total of 79 sections was reconstructed as described above. The maximum intensity projection image was reconstructed based on the data. In the parallel volume rendering method [6, 7], 3D-CTA was created by selecting the data set using a climbing slope curve with a threshold range of 95 HU (0% opacity level) to 105 HU (100% opacity level), and represented the intra-luminal contrast filling images of the vessel and cerebral aneurysm.

Case 1. (66-year-old; male; unruptured left internal carotid-posterior communicating artery aneurysm represented in Fig. 1)

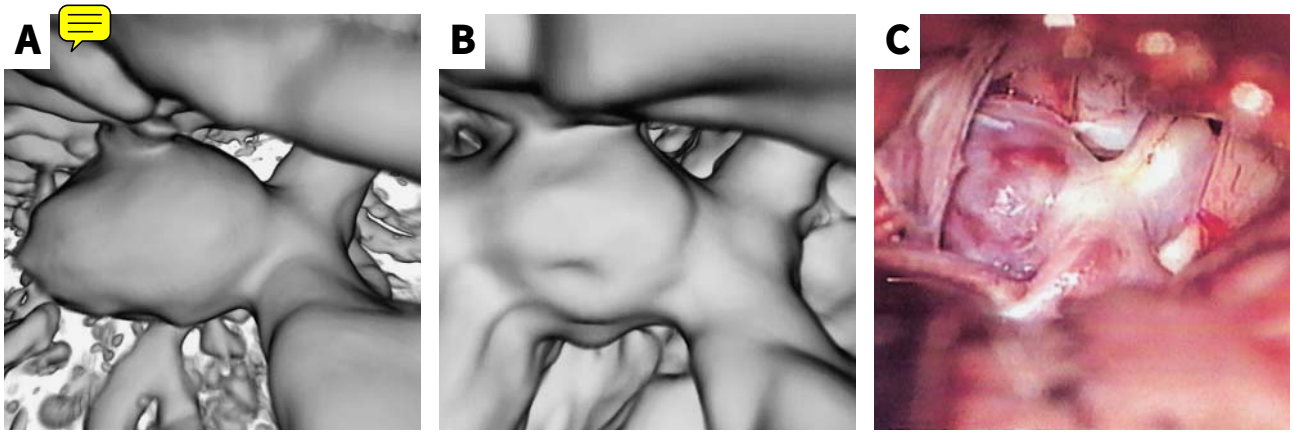

Fig. 1 Case 1. A 66-year-old man with an unruptured left IC-PC aneurysm. **A**, Three-dimensional CT angiogram showing a berry aneurysm arising from bifurcation left internal carotid artery and posterior communicating artery. **B**, Three-dimensional CT cisternogram demonstrating the irregular shape in the surface of aneurysmal dome. **C**, Surgical view confirms the similar shape of aneurysmal dome showed by three-dimensional CT cisternogram.

The patient visited our hospital complaining of a headache and requesting for further examination. During the examination of the cerebro-vascular system by MRA, an unruptured left internal carotid artery aneurysm was detected. A berry aneurysm arising from the bifurcation between the internal carotid artery and the posterior communicating artery was clearly identified by 3D-CTA (Fig. 1A). We informed the patient of the treatment options for the aneurysm. As he decided to undergo the surgical option, surgery was employed and neck clipping for the aneurysm was carried out successfully. The 3D-CTC configuration (Fig. 1B) was similar to the surgical view of the aneurysm (Fig. 1 C). The irregular surface of the aneurysmal dome in the 3D-CTC image was remarkably similar to surgical findings, thus confirming the usefulness of 3D-CTC as preoperative information.

Case 2. (77-year-old; male; unruptured right MCA aneurysm represented in Fig. 2)

Four years previously, an unruptured cerebral aneurysm in the right middle cerebral artery had been detected in the patient by MRA, but the aneurysm was left untreated and the subsequent course was observed. A berry aneurysm was detected at the M1–2 junction of the right middle cerebral artery by 3D-CTA (Fig. 2D). Additionally, stenotic lesions were detected at M1 and M2 of the parent arteries. The transparent 3D-CTC (Fig. 2E) showed the aneurysm and its parent arteries in relation to the frontal and temporal cerebral surface adjacent to the sylvian fissure. Unlikely with the 3D-CTA findings, however, the aneurysm appeared simply as a semispherical feature on 3D-CTC. Moreover, the stenotic lesions at M1 and M2 shown on 3D-CTA were not identified on 3D-CTC. In this case, comparing the 3D-CTC (Fig. 2E) to the 3D-CTA (Fig. 2D) image, the discrepancy in the wall configuration at the distal end of the aneurysmal dome at the start of the M2 superior branch was represented and might be due to arteriosclerosis or a partial thrombus formation within the aneurysm.

The patient was placed under observation without surgery, because we could not get the agreement of the surgery.

Case 3. (66-year-old; male; unruptured left MCA aneurysm represented in Fig. 3)

The patient was treated for further examination of an episode of severe headache. According to the MR angiography, a small cerebral aneurysm in the left middle cerebral artery was suspected. The 3D-CTC (Fig. 3 C) and the 3D-CTA (Fig. 3D) revealed the contour of the aneurysm's angioarchitecture and an aneurysm of 2.5 mm in size at the bifurcation of the left middle cerebral artery. The routine volume rendering 3D-CTC depicted the outer wall of the aneurysm, including parent arteries in the cistern. However, the shape of the aneurysm and parent arteries was obscured by the overlying cerebral parenchyma surrounding the sylvian fissure. To overcome the above problem, transparent 3D-CTC (Fig. 3E) was employed to visualize the vascular structures, including the aneurysmal dome, aneurysmal neck, and parent artery through the cerebral surface adjacent to the sylvian fissure. As a result, the spatial relationship between the aneurysm and the surrounding structures was delineated extensively. In this case, prophylactic surgery is being considered.

Discussion

According to intraoperative findings, Mizoi *et al.* [4] have observed the thin-walled portions with transparent red blood flow through the dome in many cases of unruptured cerebral aneurysms during aneurysmal microsurgery. They recommend a radical indication of surgical treatment, even in cases of small aneurysms. Asari *et al.* [1] also reported the contour of aneurysm by intraoperative observation. There were no reports described the contour of aneurysmal dome and neck of unruptured aneurysm preoperatively. Hashimoto *et al.* [3] reported their findings of a wall image of cerebral aneurysm using the 3D-CTA surface rendering method. In the report, they showed the discrepancy between the findings angiography and 3D-CTA.

In the present study, the region with the CT HU lower than the subarachnoid cerebrospinal fluid, enhanced by the contrast medium, was selected from the volume data set of CTC, with the 3D-CTC being reconstructed by the parallel volume rendering method. The 3D-CTC delineates the contour of the vessels and aneurysm within the cistern in relation to the surrounding brain parenchyma. Furthermore, a transparent 3D-CTC was created by extracting the boundary between the cisternal cerebrospinal fluid and the intra-cisternal structures, including vessel and aneurysm. The transparent 3D-CTC represented the expansion of the intra-cisternal architecture through overlapping structures such as the brain parenchyma and cranial base bone.

With direct visualization of the real contour of the

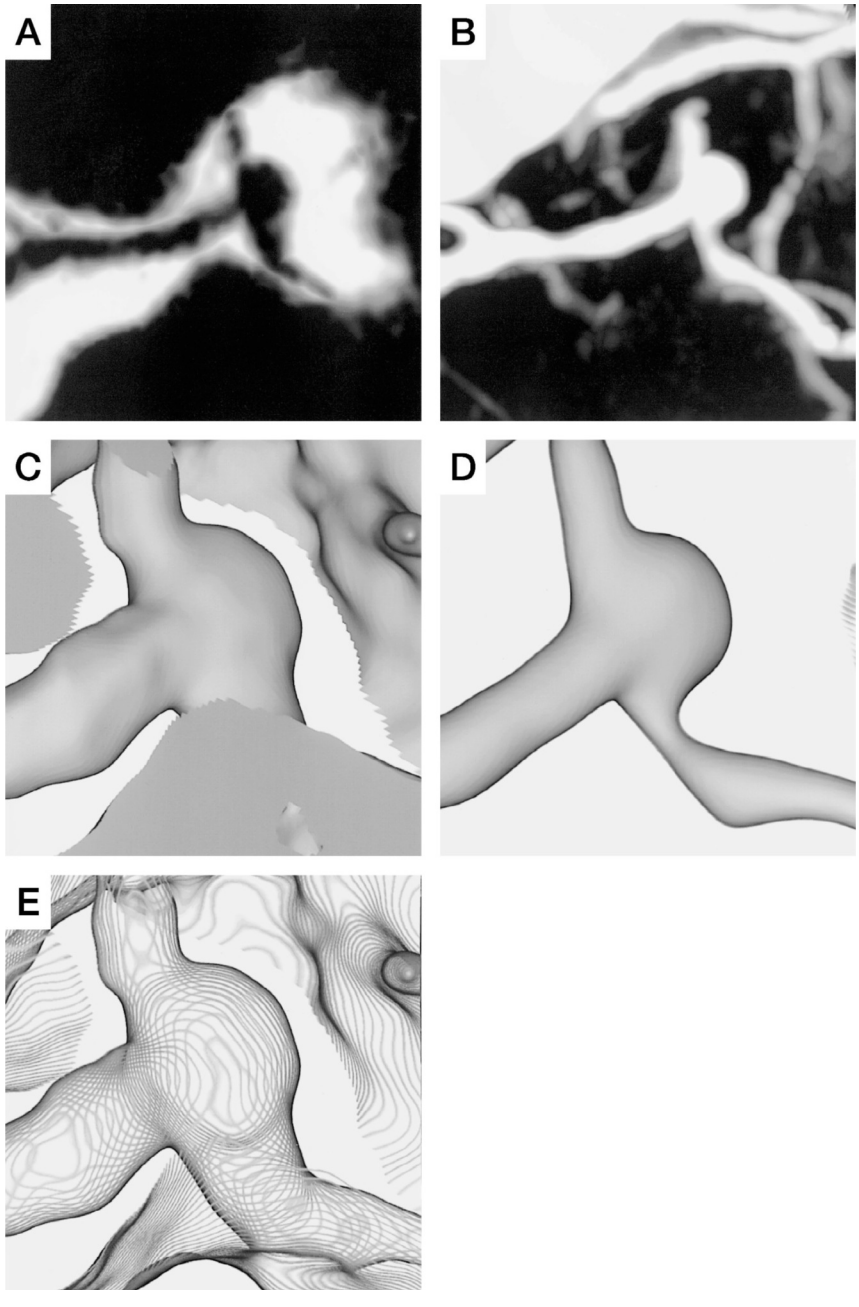

Fig. 2 Case 2. A 77-year-old man with an unruptured right middle cerebral artery aneurysm. **A**, CT cisternogram (Minimum intensity projection). The stenotic lesions at M1 and M2 were not identified on this image. **B**, CT angiogram (Maximum intensity projection) showing a berry aneurysm arose from M1-M2 junction and stenotic lesions in parent arteries. **C**, Three-dimensional CT cisternogram showing the outer wall of cerebral aneurysm, including parent arteries in the sylvian fissure. However, the shape of aneurysm and parent arteries were restricted by the obstacles of the overlying cerebral parenchyma surrounding the sylvian fissure. **D**, Three-dimensional CT angiogram showing a stenotic lesion at M2 and a berry aneurysm. **E**, Transparent three-dimensional CT cisternogram showed an extensive view of the intra-cisternal structures including cerebral aneurysm and parent arteries transparently, demonstrating a semispherical region at M1-M2 junction, unlike to the findings represented by 3D-CTA. Also brain surface adjacent to the sylvian fissure was visualized.

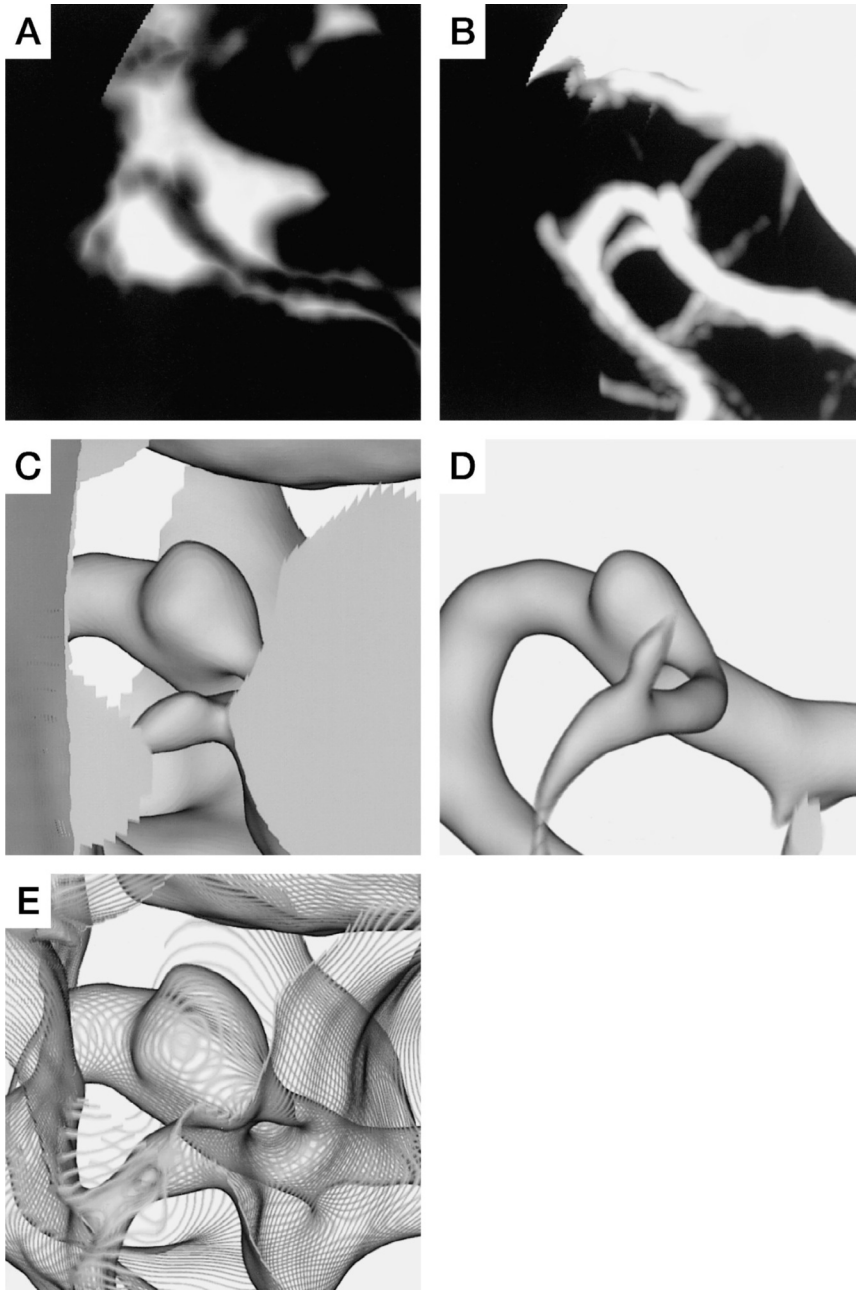

Fig. 3 Case 3. A 66-year-old man with an unruptured left middle cerebral artery aneurysm. **A**, CT cisternogram (Minimum intensity projection). **B**, CT angiogram (Maximum intensity projection) showing a berry aneurysm arose from M1-M2 junction. **C**, Three-dimensional CT cisternogram showing the outer wall of cerebral aneurysm, including parent arteries in the sylvian fissure. However, the shape of aneurysm and parent arteries were not visualized clearly because of restricting by the obstacles of the overlying cerebral parenchyma surrounding the sylvian fissure. **D**, Three-dimensional CT angiogram showing and a berry aneurysm arose from M1-M2 junction. **E**, Transparent three-dimensional CT cisternogram demonstrating a outer wall of aneurysmal dome and brain surface adjacent to the sylvian fissure was visualized extensively.

vessel and aneurysm, we used 3D-CTC for the preoperative evaluation of unruptured cerebral aneurysm. In Case 1, the aneurysm represented by the 3D-CTC was found to be remarkably similar in shape that observed in the surgical view. Our results confirm that the 3D-CTC configuration is close to the true surgical view and is useful as preoperative information. In Case 2, there was an apparent difference in the shape of the cerebral aneurysm between 3D-CTA and 3D-CTC. The 3D-CTA represented the shape of a typical berry aneurysm, and appropriate treatment was considered to include clipping of the aneurysmal neck. The 3D-CTC, however, showed a semispherical region at the distal neck extending to the beginning of the superior branch of the M2, thus making clipping of the aneurysmal neck difficult to achieve. The discrepancy in shape of the 3D-CTA and 3D-CTC views of cerebral aneurysm might be indicative of the wall thickness of the vessel and cerebral aneurysm. In this respect, intra-luminal stenosis of the parent artery due to arteriosclerosis and/or thrombus formation within the cerebral aneurysm was hypothesized. In Case 3, a subtle discrepancy in shape was shown. But we could not define the wall-thickness strictly by present technique. We considered the prophylactic surgery.

One of the problems in both 3D-CTA and 3D-CTC, the concentration of the filled contrast medium within the lumen or cistern differs among individuals and/or according to the conditions of examination, so that the CT values to defining the vessel and aneurysm boundaries are inconsistent. Additionally, the dimensions of the cerebral aneurysm are variable depending on the setting of the CT threshold. Therefore, we need further study to get much more strict data. But this approach might have high possibility to evaluate the contour of aneurysmal dome and neck.

The present study showed the contours of unruptured cerebral aneurysms preoperatively by 3D-CTC. Further study of the various cases is needed to confirm the correlation between 3D-CTC and surgical findings. But this examination is basically invasive, we also try the further study using not only CT but also MRI. The 3D-CTC may represent the useful preoperative informations which are the anatomical structure around aneurysm and the contour of aneurysmal dome and neck. We may be able to decide the surgical approach and know the shape of aneurysmal neck preoperatively. Furthermore, we believe that preoperative evaluation of the contour and the wall thickness of an unruptured cerebral aneurysm might provide useful information in the decision-making process regarding prophylactic surgery for these unruptured cerebral aneurysms.

References

1. Asari S and Ohmoto T: Growth and rupture of unruptured cerebral aneurysms based on the intraoperative appearance. Acta Med Okayama (1994) 48: 257–262.
2. Harbaugh RE, Schlusselberg DS, Jeffery R, Hayden S, Cromwell LD, Pluta D and English RA: Three-dimensional computed tomographic angiography in the preoperative evaluation of cerebrovascular lesions. Neurosurgery (1995) 36: 320–327.
3. Hashimoto H, Iida J, Hironaka Y, Shin Y and Sakai T: Wall imaging of cerebral aneurysms with a modified surface-rendering technique of spiral CT. Acta Neurochir (Wien) (2000) 142: 1003–1012.
4. Mizoi K, Yoshimoto T and Nagamine Y: Types of unruptured cerebral aneurysms reviewed from operation video-recordings. Acta Neurochir (Wien) (1996) 138: 965–969.
5. Murayama Y, Sakurama K, Satoh K and Nagahiro S: Identification of the carotid artery dural ring by using three-dimensional computerized tomography angiography. J Neurosurg (2001) 95: 533–536.
6. Rubin GD, Beaulieu CF, Argiro V, Ringl H, Norbash AM, Feller JF, Dake MD, Jeffrey RB and Napel S: Perspective volume rendering of CT and MR images: Applications for endoscopic imaging. Radiology (1996) 199: 321–330.
7. Satoh T: Transluminal imaging with perspective volume rendering of computed tomographic angiography for the delineation of cerebral aneurysms. Neurol Med Chir (Tokyo) (2001) 41: 425–430.
8. Schievink WI, Piepgras DG and Wirth FP: Rupture of previously documented small asymptomatic saccular intracranial aneurysms. Report of three cases. J Neurosurg (1992) 76: 1019–1024.
9. Yasui N, Suzuki A, Nishimura H, Suzuki K and Abe T: Long-term follow-up study of unruptured intracranial aneurysms. Neurosurgery (1997) 40: 1155–1160.